ACSNANO

www.acsnano.org

ARTICLE

Sensing Capabilities of Single Nanowires Studied with Correlative *In Situ* Light and Electron Microscopy

Lilian M. Vogl, Peter Schweizer, Peter Denninger, Gunther Richter, and Erdmann Spiecker*

Cite This: *ACS Nano* 2022, 16, 18110–18118

Read Online

ACCESS | Metrics & More | Article Recommendations | Supporting Information

ABSTRACT: **Modern devices based on modular designs require versatile and universal sensor components which provide an efficient, sensitive, and compact measurement unit. To improve the space capacity of devices, miniaturized building elements are needed, which implies a turning away from conventional microcantilevers toward nanoscale cantilevers. Nanowires can be seen as high-quality resonators and offer the opportunity to create sensing devices on small scales. To use such a one-dimensional nanostructure as a resonant cantilever, a precise characterization based on the fundamental properties is needed. We present a correlative electron and light microscopy approach to characterize the pressure and environment sensing capabilities of single nanowires by analyzing their resonance behavior *in situ*. The high vacuum in electron microscopes enables the characterization of the intrinsic vibrational properties and the maximum quality factor. To analyze the damping effect caused by the interaction of the gas molecules with the excited nanowire, the *in situ* resonance measurements have been performed under non-high-vacuum conditions. For this purpose, single nanowires are mounted in a specifically designed compact gas chamber underneath the light microscope, which enables direct observation of the resonance behavior and evaluation of the quality factor with dependence of the applied gas atmosphere (He, N_2, Ar, Air) and pressure level. By using the resonance vibration, we demonstrate the pressure sensing capability of a single nanowire and examine the molar mass of the surrounding atmosphere. Together this shows that even single nanowires can be utilized as versatile nanoscale gas sensors.**

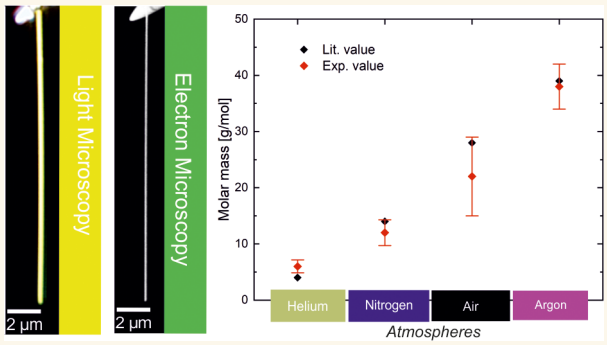

KEYWORDS: *correlative in situ microscopy, nanowire, resonance, quality factor, sensing*

Microcantilevers[1−3] are already successfully implemented in mass sensing devices, offering a sensitivity down to the subpicogram range.[4−6] The performance of such a cantilever based device depends on the resonance frequency and sharpness of the resonance peak, i.e., quality factor.[7,8] While for mass sensing applications the frequency shift is used,[9,10] the corresponding quality factor additionally depends on the ambient medium and scales inversely with the pressure in the measurement regime.[11,12] Cantilevers have also been used for pressure sensing, however, their applicable pressure range[13] is restricted by their dimensions. To expand the pressure range, the size of the cantilevers has to be further reduced: A beam with a thickness in the nm range can significantly broaden the measurable range and further shift it to higher values.[7] Cantilevers produced by microfabrication technology[14] are difficult to make sufficiently small while maintaining a high enough quality. One potential alternative is nanowires, which can have a very small size while being single-crystalline with a low defect concentration. Such metallic nanowires can be produced by physical vapor deposition,[15,16] electrodeposition,[17] or indirect means via a thermally induced conversion mechanism.[18]

However, a drawback of nanowires is that their cross-sectional shape[19] and therefore their resonance behavior can strongly vary across a batch. Therefore, a precise characterization of the vibrational properties of nanowires is required before they can be used for sensing. The analysis of the individual nanowire properties is essential to create functional

Received: May 17, 2022
Accepted: October 5, 2022
Published: October 25, 2022

https://doi.org/10.1021/acsnano.2c04848
ACS Nano 2022, 16, 18110−18118

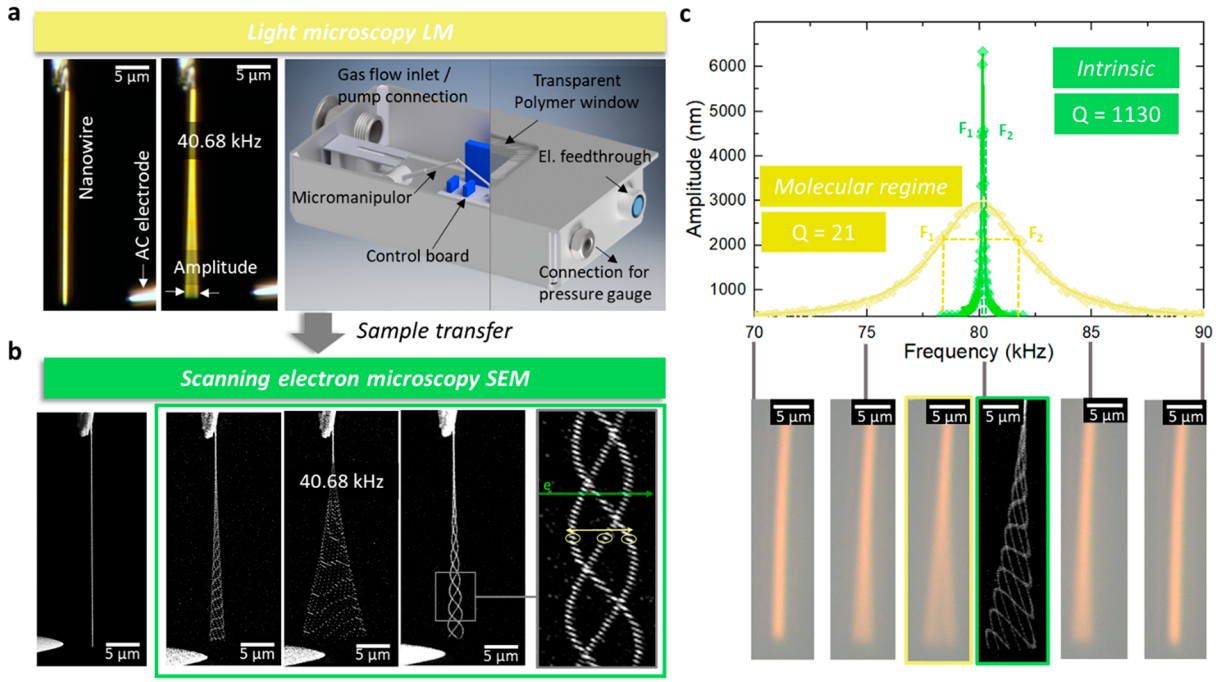

Figure 1. Illustration of the experimental setup and workflow. In order to analyze the vibrational properties of a single nanowire under different conditions, the resonance measurements (via electrical excitation) are performed correlatively in SEM and LM. (a) Setup for the light microscopy study. The nanowire is attached to a micromanipulator mounted in a compact gas chamber underneath the light microscope. The electrical excitation is realized with a metal tip (AC electrode) attached to a second micromanipulator. The frequency sweep revealed the largest oscillation amplitude (directly observable in the LM image) at the resonance frequency of 40.68 kHz. (b) Subsequently, the sample is transferred to the SEM, where correlative resonance measurements are performed (green box: images taken during frequency sweep). The resonance frequency is again at 40.68 kHz. The SEM images show an interference pattern of the scanning electron beam and the oscillating nanowire. (c) Exemplary comparison of resonance curves in LM and SEM of a different wire. In SEM, the nanowire reveals a sharp resonance at 80.1 kHz with a high intrinsic quality factor of Q = 1130. The resonance curve recorded in LM at a pressure of 120 mbar (ambient air) shows a much broader resonance curve corresponding to a strongly reduced extrinsic quality factor of Q = 21.

arrays which can be further integrated in next-generation sensing devices.[20,21] Several sensitivity records regarding mass,[22] gas concentration,[23] or force[24] based on single nanoresonators have already been reported showing the great potential of nanowires. However, the precise microscopic analysis of the vibrational behavior on small scales and in different environments is still pending.

In this study, we demonstrate the sensing capabilities of single nanowires by using correlative *in situ* light and electron microscopy. The ability to observe one-dimensional nanostructures with light optical methods offers the opportunity to characterize the vibrational behavior not only in a vacuum but also under realistic application of related conditions. The damping arising from intrinsic and extrinsic effects can be described by the quality factor of the resonance vibration. The intrinsic quality factor[25] crucially depends on the microstructure and surface quality of the nanowire. Our correlative analysis in the electron microscope with idealized high-vacuum conditions enables the clear assignment of intrinsic nanowire properties. The extrinsic damping observed underneath the light microscope can be attributed to the interaction of the gas molecules with the vibrating nanocantilever[26] and depends on the pressure and the type of the surrounding atmosphere. Our comprehensive study introduces an innovative microscopy setup to characterize the quality factor on small scales and reveals the pressure and gas sensitive resonance behavior of single nanoscale cantilevers.

RESULTS

Resonance Measurements and Quality Factor Analysis. To analyze the vibration properties of a single nanowire in dependence of the surrounding environment, resonance measurements are performed *in situ* in light microscope LM and scanning electron microscope SEM. The general setup for resonance measurements is universal and independent of the ambient medium. Depending on whether the experiment is performed in a high vacuum (SEM) or at higher pressures (LM), the sharpness of the resonance peak and therefore the quality factor changes.[27] The dimensionless quality factor Q is defined by the resonance frequency $F_{\mathrm{Resonance}}$ and the bandwidth $F_2 - F_1$:

$$Q = \frac{F_{\mathrm{Resonance}}}{F_2 - F_1} \tag{1}$$

For a resonance curve, F_1 and F_2 describe the frequencies, where $1/\sqrt{2}$ of the maximum attainable amplitude A_{max} is reached. For both setups in SEM and LM, electrical excitation[28] is used to excite the resonance with defined frequency and to further perform frequency sweeps. To achieve this, an electrode is arranged perpendicular to the sample (see Figure 1) and a waveform generator applies a sinusoidal AC voltage. By sweeping through the appropriate frequency range, the resonance vibration with maximum amplitude can be detected. The maximum amplitude depends on several factors such as electrode−wire distance and applied

https://doi.org/10.1021/acsnano.2c04848
ACS Nano 2022, 16, 18110−18118

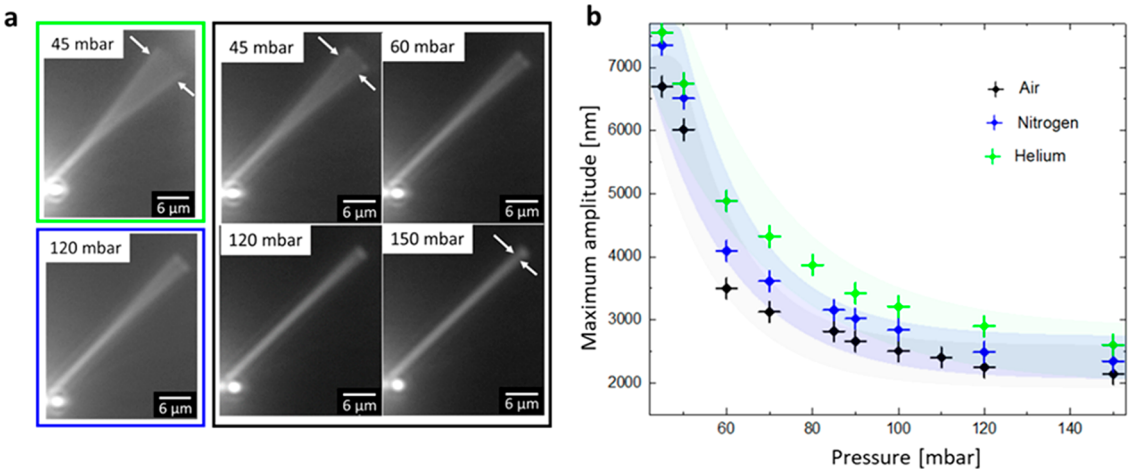

Figure 2. Pressure dependent resonance behavior. (a) Some exemplary LM images (greyscale) used for the evaluation. (b) Maximum amplitude at the resonance frequency of 21.7 kHz with increasing pressure for different atmospheres (ambient air, nitrogen, helium).

AC voltage. However, the calculation of the quality factor is not affected by a changing maximum amplitude as it is solely based on the shape of the resonance peak.

For our study we used PVD grown gold nanowires with high structural quality.[15] To perform resonance measurements, freestanding conductive nanowires are required, so that they can vibrate freely and can respond to the applied AC voltage. During preparation of the correlative experiments, several nanowires have been attached to tungsten tips in advance. In SEM and LM, a fixed micromanipulator setup consisting of two manipulators is used, which allows a precise alignment of the nanowires with respect to the second electrode tip. Figure 1 illustrates the resonance measurements in LM and SEM and the correlative workflow. To avoid any effect of contamination of the nanowire by long-term electron beam imaging, resonance measurements were first performed in the light microscope and subsequently in the electron microscope. Additionally, the exposure to the electron beam was limited by using short-term exposures and low currents (<100 pA).

Correlative *In Situ* Light and Electron Microscopy. Despite the small scale, nanowires and their resonance behavior can be imaged and analyzed under certain conditions with LM (see Supporting Information 1). The resolution of a conventional light microscope is in the range of ∼400 nm[29] and is given by the diffraction limit according to the Abbe[30] or Rayleigh criterion.[31] The Rayleigh criterion states that, depending on the wavelength λ of the light source and the numerical aperture NA of the objective lens, two object points are separated in the image if their distance exceeds 0.61 λ/NA. In this study, we analyzed nanowires with a thickness in the range 180−350 nm and lengths of 25−38 μm. Even though the thickness of the nanowires is below the resolution limit, the nanowires are clearly revealed in the LM images since they occur as isolated nanowires in the resonance setup. The nanowire contrast is broadened by the point spread function of the optical system but this does not hinder the analysis of nanowire resonance which adds additional broadening (Figure 1c, bottom). If the resonance amplitude exceeds the resolution limit, even two separated nanowire images appear since the contrast is dominated by the turning points of the oscillation. By evaluating the broadening of the contrast at the nanowire tip, the resonance amplitude can be determined as a function of the excitation frequency. From the resulting resonance curve the quality factor can be extracted with high precision, as demonstrated by Figure 1c (top). To analyze the resonance behavior of single nanowires under different gas atmospheres and pressure conditions, a compact pressure chamber for the light microscope was developed; see Figure 1a. The chamber (stainless steel, wall thickness 3 mm) allows a minimum pressure of 10 mbar and a polymer window enables the *in situ* observation of the resonance vibration. For the experiment, long working distance objectives with a numerical aperture of 0.6 and magnification of 50× are used. After completion of the LM experiments, the nanowire sample is transferred to the SEM where correlative resonance sweeps are performed; see Figure 1a,b. While in the light microscope a smooth broadening of the nanowire contrast during frequency sweep is observed, the SEM images show an interference pattern of the scanning electron beam and the oscillating nanowire. Figure 1c compares exemplarily correlative data for a nanowire obtained in the light microscope (120 mbar, ambient air) and SEM (10^{-6} mbar). The maximum of the resonance peak is located at 80.1 kHz and is independent of the pressure condition. However, the quality factor and therefore the sharpness of the resonance behavior changes with the pressure. In SEM, the intrinsic quality factor Q is measured to be 1130. The resonance measurement in the light microscope shows a much broader resonance peak corresponding to a quality factor of $Q = 21$. This changing quality factor forms the basis for the sensing capabilities of the nanowire.

Gas Flow Regimes Defined by the Knudsen Number. Depending on the pressure level, different effects of a surrounding gas on a vibrating beam have to be taken into account. The gas flow regimes are defined according to the Knudsen number K_n, which depends on the mean free path λ and the width of the cantilevered beam w:

$$K_n = \frac{\lambda}{w} \tag{2}$$

Conventionally, $K_n > 10$ signifies the free molecular flow regime with a transition zone between $10 > K_n > 0.01$ and finally a continuum flow in $0.01 < K_n$.[12] Depending on the cantilever size and geometry, the exact transition of the molecular to the continuum regime can vary.[32] Based on our measurement we define interaction regions for our nanocantilever with the gas molecules (see Supporting Information 2).

https://doi.org/10.1021/acsnano.2c04848
ACS Nano 2022, 16, 18110−18118

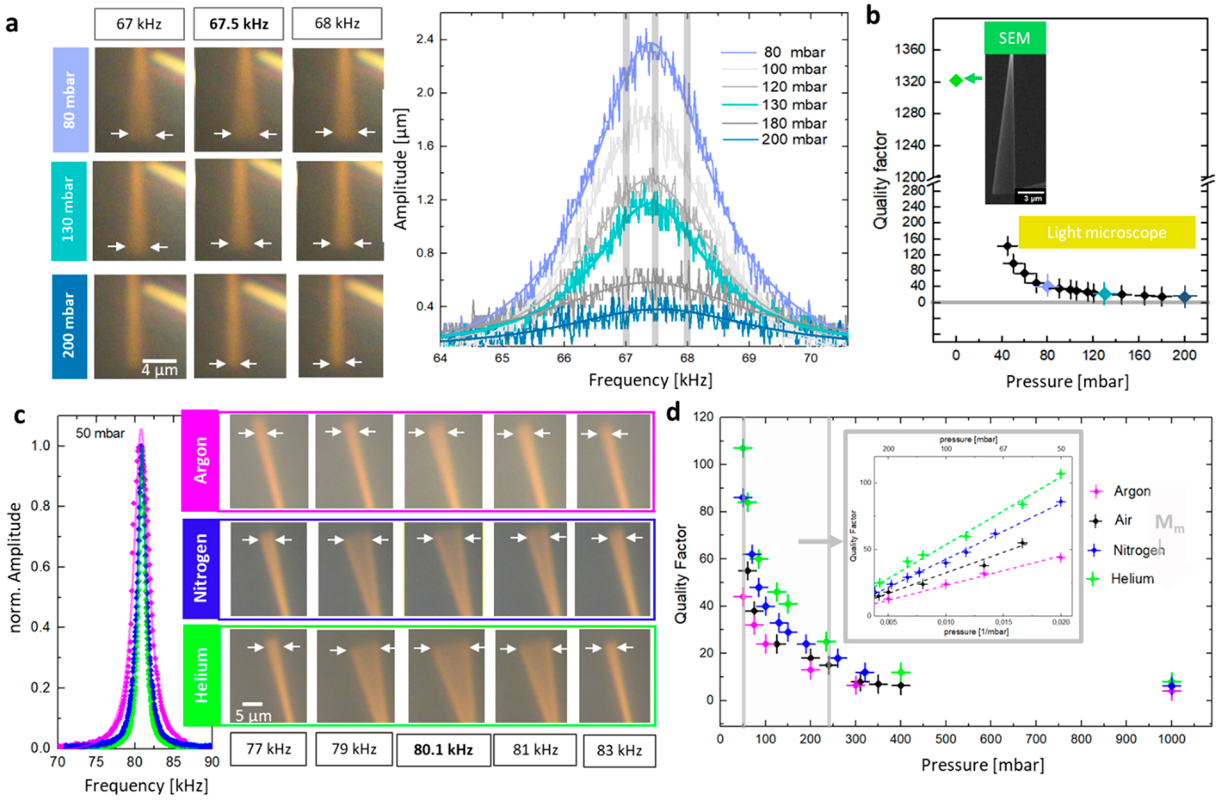

Figure 3. Quality factor analysis. Pressure dependent resonance behavior: (a) Resonance curves for different pressure levels (ambient air) and exemplary LM images at the resonance frequency 67.5 kHz and at 67 kHz/68 kHz. (b) Corresponding *Q* factor analysis with dependence on the pressure. Inset: SEM image at the resonance frequency and the highest quality factor. Effect of the gas atmosphere on the nanowire vibration: (c) Exemplary LM images at the resonance frequency $F_{Resonance}$ = 80.1 kHz and nearby frequencies (50 mbar). The plot on the left side compares the normalized resonance curves for different gas environments (helium, nitrogen, argon). (d) Measured quality factor with dependence on the pressure and the gas environment. Gray shaded area: measurement region. Inset: Linear relationship of quality factor and inverse pressure (1/mbar).

The high vacuum in the SEM gives us access to the intrinsic region ($K_n \gg 10$), where the influence of gas molecules on the beam vibration can be neglected.[33] Hence, the sharpness of the nanowire vibration only depends on the intrinsic properties like the surface quality and microstructure. Within our measurement region ($10 > K_n > 1$), the interaction of the gas molecules with the vibrating beam cannot be further neglected and the damping of the beam scales directly with the pressure.

Maximum Amplitude. As described above, the resonance frequency of the nanowire is located at the maximum vibrational amplitude (for one vibrational mode[19]). The quality factor is independent of the actual amplitude, which depends on the strength of excitation and is a universal parameter to compare different resonance data. However, the information on the maximum amplitude can be used as an illustrative tool to examine the pressure dependent resonance behavior of a single nanowire. Providing the same excitation conditions during repeated frequency sweeps at different pressure levels, the changing maximum amplitude at the resonance frequency can directly be observed. Figure 2 compares the attained amplitude at the resonance frequency $F_{resonance}$ = 21.7 kHz and shows the corresponding exemplary LM images used for the evaluation. Staying at the resonance frequency, the pressure (45−150 mbar) has been increased in order to directly observe *in situ* the effect on the resonance amplitude. In general, the nanowire shows the same pressure-dependent behavior in different gas environments: At the lowest set pressure value of 45 mbar, the nanowire has the maximum resonance amplitude. Increasing the pressure reduces the resonance amplitude significantly. After reaching 120 mbar, the maximum vibration amplitude tends toward a constant value. The decreasing amplitude in dependence of the pressure already indicates the impact of the gas molecules on the nanowire oscillation. The nanowire reaches the highest amplitude in helium atmosphere and the lowest one in ambient air.

Quality Factor Analysis: Pressure Dependency and Effect of the Used Gas Atmosphere. To gain more information about the pressure dependent resonance behavior, complete frequency sweeps over the resonance peak are recorded. Figure 3a compares the resonance curves of a nanowire recorded at different pressure levels (ambient air). At the frequency $F_{resonance}$ = 67.5 kHz the maximum resonance peak is reached. To illustrate the symmetric vibration, light microscopic images at $F_{resonance}$ and at nearby frequencies (67 kHz/68 kHz) are shown. At 80 mbar, the resonance vibration of the nanowires is clearly revealed with a maximum amplitude of 2.4 μm. At 130 mbar, the amplitude already decreases significantly resulting in a value of 1.2 μm at resonance frequency. By increasing the pressure further to 200 mbar the vibration at resonance is reduced to the smallest detected value of 400 nm. To analyze such small beam deflections precisely, an automated image analysis routine (implemented in Python) has been introduced which evaluates line profiles across the vibrating nanowire at the nanowire tip (Supporting Informa-

https://doi.org/10.1021/acsnano.2c04848
ACS Nano 2022, 16, 18110−18118

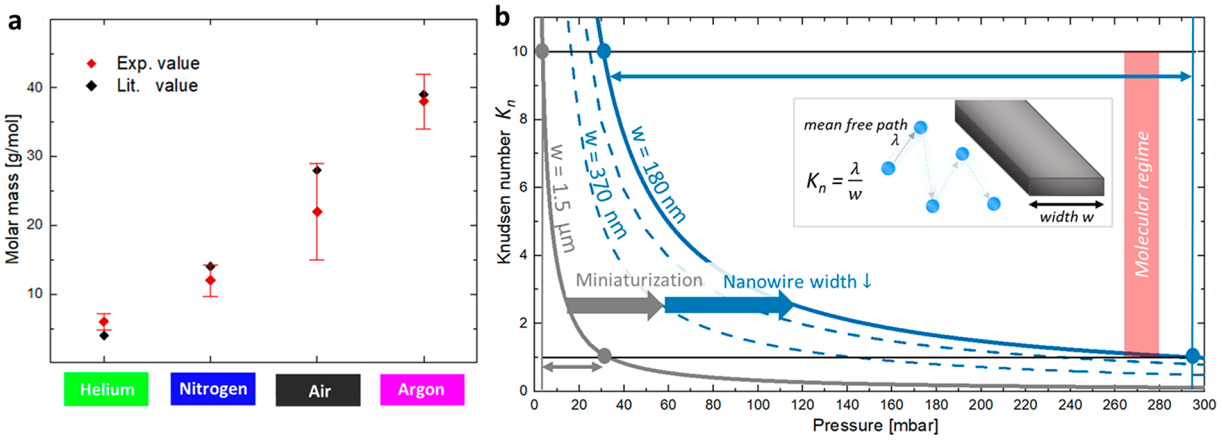

Figure 4. Demonstration of the gas and pressure sensing capability of single nanowires based on resonance vibrations. (a) Molar mass of the gas molecules extracted from the measurements in Figure 3 using the Christian model (eq 4) and comparison with the theoretical values showing excellent agreement. (b) Effect of the beam width on the gas-sensitive pressure regime. For the calculation the collision diameter of air is used.

tion 3). The trend of a decreasing resonance amplitude and the complete quality factor analysis (see Figure 3a) illustrate the pressure dependent vibration behavior of the nanowire. The correlative resonance measurement of the nanowire in the SEM reveals a quality factor Q = 1320 within the intrinsic region. In the light microscopy setup (45−200 mbar), a clear trend for the quality factor with increasing pressure is observed. The trend of a decreasing quality factor with increasing pressure is not only observed for ambient air but also for other gas environments. However, the impact of the gas molecules on the nanowire vibration depends on their molar mass. Figure 3c compares exemplarily the effect of the different gas molecules on the beam vibration at the same pressure of 50 mbar. The resonance frequency of the nanowire is located at $F_{Resonance}$ = 80.1 kHz, which is also confirmed by the complementary resonance measurement in the SEM. The LM images show the symmetrical shape of the resonance peak. In a helium atmosphere, the resonance vibration of the nanowire is clearly visible with a high maximum amplitude. In an argon atmosphere, the nanowire vibration is significantly suppressed and the resonance peak is broadened. The quality factor analysis at 50 mbar reveals values of Q_{Helium} = 110 in helium and Q_{Argon} = 42 in argon, respectively. In a nitrogen atmosphere, the quality factor shows an intermediate value of $Q_{Nitrogen}$ = 90. The intrinsic quality factor of the nanowire is subsequently measured in the SEM resulting in a value of Q_{SEM} = 1130. Figure 3d summarizes the pressure dependent quality factors for the different environments. With increasing pressure, the quality factor decreases and finally tends toward a constant value. The relative values of the quality factors depend on the gas environment. Helium has a low molar mass of 4 g/mol, compared to argon with 40 g/mol. Therefore, the sharpness of the resonance peak differs for each gas atmosphere. In helium, the highest values for the quality factor are reached. In argon at the same respective pressure level, the resonance peak is broader with a much lower quality factor. By plotting the measured quality factors as a function of the inverse pressure (in 1/mbar), a systematic trend becomes visible; see the inset in Figure 3d. Here, only pressure values from the gray shaded area are taken into account, corresponding to the measurement region of the nanowire. Within this pressure range of around 50−250 mbar, an inverse linear relationship of the pressure to the quality factor can be observed. In the molecular gas flow regime, the collisions of the molecules with the beam crucially affect the oscillating motion of the nanowire. The corresponding damping strongly depends on the molar mass of the gas molecules, which is reflected in the absolute values of the quality factor but also in different slopes of the curve. Below 50 mbar, the quality factor increases significantly, indicating the transition to the intrinsic region. At around 300 mbar, the quality factor converges toward a constant value.

DISCUSSION

The total quality factor of the nanowire constitutes itself by the intrinsic ($Q_{intrinsic}$) and the extrinsic factors ($Q_{extrinsic}$):[25]

$$\frac{1}{Q} = \frac{1}{Q_{intrinsic}} + \frac{1}{Q_{extrinsic}} \tag{3}$$

Using the intrinsic quality factor $Q_{intrinsic}$ obtained in SEM and the measured total quality factor, the extrinsic quality factor $Q_{extrinsic}$ can be calculated. In the following section, the extrinsic quality factor is used to demonstrate the gas and pressure sensing capability of single nanowires. Moreover, the intrinsic effects on the quality factor are discussed.

Extrinsic Effects. The reason for the gas dependent resonance behavior can be explained by the colliding gas molecules with the nanobeam. A gas molecule with a high molar mass has a strong damping effect on the oscillating motion of the beam. With decreasing molar mass the observed damping effect gets weaker. This direct correlation between the type of gas molecule, the pressure and the quality factor is generally the foundation for sensing applications based on resonance vibrations. Within the molecular flow regime, the Christian model[34,35] can be used to describe the resonance behavior of a cantilevered beam:

$$Q_{mol} = \left(\frac{\pi}{2}\right)^{3/2} \frac{\sqrt{R_0 T / M_m}}{P} w \rho f \tag{4}$$

The quality factor Q_{mol} depends on beam specific parameters (beam width w, density ρ, resonance frequency f), as well as on the pressure P and the molar mass M_m of the surrounding atmosphere. The effect of gas temperature T enters through the thermal energy term R_0T with the universal gas constant R_0 = 8.314 J/kmol. In the course of the last years, several other

https://doi.org/10.1021/acsnano.2c04848
ACS Nano 2022, 16, 18110−18118

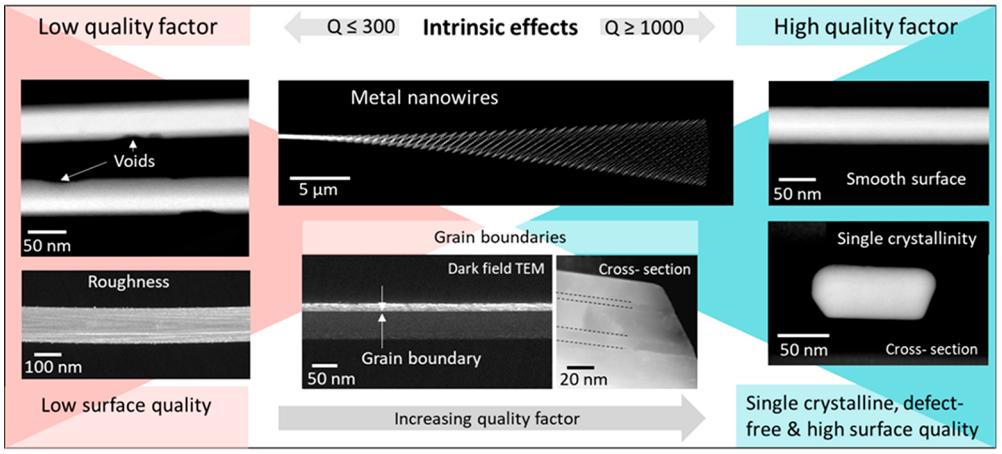

Figure 5. Illustration of the impact of microstructure and surface quality (intrinsic effects) on the intrinsic quality factor of metal nanowires. Representative STEM images of metal nanowires. Low quality factors are observed for nanowires, which show inhomogeneities and voids on the surface. In contrast to that, high quality factors are achieved with single crystalline nanowires, which show a smooth surface. Defect structures like twin grain boundaries also affect the intrinsic quality factor, however, not as much as the surface quality.

models[36,37,26] have been proposed. However, the Christian model has been successfully applied as a universal simple approach[38] and several independent experiments have proven its applicability to describe the beam behavior on large scales.[32,13] By going down to smaller scales and using nanowires as the resonating beam structure, the dimension of the beam changes from mm to nm. However, the quality factor is still influenced by the atmospheric (pressure/gas) conditions.

To verify our measured quality factors and to prove the gas sensing capability of the single nanowire, we applied the Christian model in order to extract the molar mass from our experimental data. The resulting values are depicted in Figure 4a and are compared to the calculated values for the different environments showing good agreement. For this calculation, a wire with a width of 295 nm was used. The width was estimated in SEM by tilting the wire so that the actual area interacting with the gas molecules is visible. The mean values are obtained by calculating the molar mass for the different pressure−quality factor pairs and then taking the average. The error bars are based on the standard deviation of those experiments. The calculation of the molar mass is limited by experimental uncertainties (discussed in Supporting Information 4) as well as shortcomings in the Christian model. Nevertheless, our experiment demonstrates that the effect of damping caused by the gas molecules can be used for sensing even with single nanowires.

This is of key interest since the nanoscale dimension of the cantilever beam significantly increases the gas-sensitive pressure range as illustrated in Figure 4b. Decreasing the size of the resonating beam leads to a shift and broadening of the sensitive range. As described above, the Knudsen number depends on the beam width and the mean free path, which is a specific value describing the atmospheric conditions. While we can adapt the beam dimensions by choosing a specific nanowire, the mean free path λ is given by the pressure P and the collision diameter d of the gas molecule:

$$\lambda = \frac{k_B T}{\sqrt{2}\,\pi d^2} \cdot \frac{1}{P} \tag{5}$$

with the Boltzmann constant k_B and the temperature T. For example, under normal pressure (~1000 mbar) with a collision diameter of $d_{air} = 4.19 \times 10^{-10}$ m,[32] the mean free path is given by $\lambda = 66$ nm.[39] To achieve a molecular gas flow under these conditions, the beam width has to be of the same size or even smaller, meaning $w \leq 66$ nm. By using nanowires, these beam widths can be achieved and the sensing capable pressure range can be extended to higher values. In Figure 4b, the sensing range for microsized cantilevers with a width of 1.5 μm is compared to the range achieved by nanowires with different widths. The nanowire (w = 180 nm; see Supporting Information 5) shows a systematic pressure and gas dependent resonance behavior between 40 and 290 mbar. The range for the microsized cantilever is more restricted and only the range between 5 and 30 mbar can be sensed, assuming the same atmospheric conditions. The range for the measurement region is shifted for different gas atmospheres, as the collision diameter changes. Therefore, helium with a small collision diameter of $d_{He} = 2.6 \times 10^{-10}$ m[40] is easier to measure up to higher pressures with resonant based sensing devices.

Intrinsic Effects. As described in the results part, the measured quality factor of the nanowires in the SEM is as high as $Q > 1000$. The resonance sharpness in a high vacuum depends on the intrinsic nanowire properties. The surface quality, like roughness or inhomogeneities, and the microstructure affect the measured quality factor in the SEM. In the course of this study, we analyzed the resonance properties of multiple metal (gold, copper) nanowires in SEM to characterize the intrinsic quality factor. Moreover, we established a workflow (Supporting Information 6), including TEM plan-view and cross-section analysis of a previously resonated nanowire to get the link between the microstructure and the observed quality factor in SEM. We observed the impact of different intrinsic effects on the quality factor of metal nanowires. Figure 5 presents our findings with exemplary STEM images and illustrates the effect on the intrinsic quality factor. In the light microscopy part of this study, we have deliberately chosen gold nanowires as the sample system. In contrast to copper, which naturally forms a native oxide layer on the surface, gold is known for its chemical inertness and stability. With our setup for resonance measurements, we observed the highest quality factors ($Q \geq 1000$) for single crystalline gold nanowires with low defect concentration, which are characterized by a high surface quality. Such gold

https://doi.org/10.1021/acsnano.2c04848
ACS Nano 2022, 16, 18110−18118

nanowires are suitable candidates for resonating devices, as their intrinsic vibrational properties enable sensing with low noise level. On the other hand, the lowest quality factors ($Q \leq 300$) are observed for nanowires with a poor surface quality (Supporting Information 7). Especially copper nanowires show a rough surface with voids and dimples. Interestingly, we see that defect structures like grain boundaries or stacking faults do not affect the intrinsic quality factor as much as the surface quality. Twin grain boundaries in metal nanowires are likely formed during the growth process. As a defect, they act as a barrier during the vibration motion and decrease the quality factor.[19] We conclude that the surface quality, including roughness and voids, has the greatest impact on the quality factor. By continuing our basic ideas, we can even think of replacing the relatively expensive material gold by transition metal oxides. As example, molybdenum oxide nanowires combine a high chemical stability with excellent mechanical properties[41] and smooth surface,[42] implying outstanding high quality factors.

CONCLUSION

As shown in the literature, nanowires have versatile application possibilities in electrical,[43,44] optical,[45,46] and sensor[47,48] devices. With this study, we demonstrate the sensing capability of single nanowires by using correlative microscopy techniques. The analysis of the resonance properties of a single nanowire is a fundamental part in creating building units for future sensing devices. In particular, it forms the basis for an in-depth understanding of functional nanowire arrays. The demonstrated ability to directly reveal and analyze the resonance behavior of single nanowires in the light microscope enables experiments for sensing studies and applications under ambient conditions. In combination with correlative electron microscopy, the intrinsic and extrinsic quality factor can be analyzed consistently for the same nanowire. Moreover, by complementing the resonance measurements with high-resolution TEM analyses the intrinsic vibrational behavior and quality factor can be related to the microstructural and surface properties of the nanowire. We show that the resonance behavior of a single nanowire observed *in situ* in the light microscope sensitively depends on the gas environment, which can be exploited for measurement of the gas pressure and molar mass of the surrounding medium. We believe that the correlative workflow devised in the present work can be used and further adapted to analyze the functionality of promising nanostructures for sensor applications.

METHODS/EXPERIMENTAL SECTION

The light microscopy experiment was done in a Nikon LV100ND microscope, equipped with a long working distance objective LWD50x. The correlative SEM experiment was done in a ThermoFischer Helios Nanolab 660 FIB/SEM. The TEM studies for the intrinsic quality factor evaluation was performed with a ThermoFischer Titan Themis3 300 TEM.

For resonance measurement, a single nanowire was attached to a tungsten tip suitable for Kleindiek MM3A-EM micromanipulators. Based on the specifications of the micromanipulators, the tips can be positioned with a resolution better than 1 nm. For each experiment (one nanowire tested in different conditions), the electrodes are kept at a constant position. Long-term drift is counteracted with minor readjustments. However, the accuracy is limited in the light microscope by the resolution. The depth of the field with the used objective is around 1 μm. Given that the wires remain in focus during vibration, we can estimate an upper limit of the rotational misorientation of about 5°. The effect of a misalignment is a change in maximum amplitude. To excite the nanowire in the resonance frequency, a waveform generator Rigol DG1022Z with a frequency range of 1 μHz to 25 MHz and a sample rate of 200 MSa/s is used. A sinusoidal wave with 2 V_{pp} is applied for excitation, and the frequency is swept through the interesting frequency range (1 μHz resolution, range normally between 1 and 200 kHz). To measure the pressure difference between the laboratory and the gas chamber, we use a mechanical differential pressure gauge from Wika (class 1.6). To obtain the absolute pressure values, we measured the ambient pressure in the laboratory using a Greisinger GMH absolute scale barometer (accuracy 2 mbar).

ASSOCIATED CONTENT

Supporting Information

The Supporting Information is available free of charge at https://pubs.acs.org/doi/10.1021/acsnano.2c04848.

SI2, schematic illustration of the gas flow regimes according to the Knudsen number and measurement regions; SI3, evaluation of the resonance frequency via automated image analysis/line profiling; SI4, error propagation for the calculation of the molar mass; SI5, effect of the nanowire width to the measurable pressure range; SI6, workflow to characterize the intrinsic quality factor (plan-view and cross-section analysis in TEM); SI7, vibration of copper nanowires (effect of surface quality on the quality factor) (PDF)

SI1, *in situ* light microscopy video of resonating nanowire (AVI)

AUTHOR INFORMATION

Corresponding Author

Erdmann Spiecker − *Institute of Micro- and Nanostructure Research (IMN), Center for Nanoanalysis and Electron Microscopy (CENEM), Interdisciplinary Center for Nanostructured Films (IZNF), Friedrich-Alexander-Universität Erlangen-Nürnberg, 91058 Erlangen, Germany;* orcid.org/0000-0002-2723-5227; Email: Erdmann.Spiecker@fau.de

Authors

Lilian M. Vogl − *Institute of Micro- and Nanostructure Research (IMN), Center for Nanoanalysis and Electron Microscopy (CENEM), Interdisciplinary Center for Nanostructured Films (IZNF), Friedrich-Alexander-Universität Erlangen-Nürnberg, 91058 Erlangen, Germany*

Peter Schweizer − *Institute of Micro- and Nanostructure Research (IMN), Center for Nanoanalysis and Electron Microscopy (CENEM), Interdisciplinary Center for Nanostructured Films (IZNF), Friedrich-Alexander-Universität Erlangen-Nürnberg, 91058 Erlangen, Germany*

Peter Denninger − *Institute of Micro- and Nanostructure Research (IMN), Center for Nanoanalysis and Electron Microscopy (CENEM), Interdisciplinary Center for Nanostructured Films (IZNF), Friedrich-Alexander-Universität Erlangen-Nürnberg, 91058 Erlangen, Germany*

Gunther Richter − *Max Planck Institute for Intelligent Systems, 70569 Stuttgart, Germany*

Complete contact information is available at: https://pubs.acs.org/10.1021/acsnano.2c04848

Author Contributions

The manuscript was written through contributions of all authors. All authors have given approval to the final version of the manuscript.

Notes

The authors declare no competing financial interest.

ACKNOWLEDGMENTS

The authors gratefully acknowledge funding by the DFG through projects GRK 1896 and SFB 953.

REFERENCES

(1) Mouro, J.; Pinto, R.; Paoletti, P.; Tiribilli, B. Microcantilever: Dynamical Response for Mass Sensing and Fluid Characterization. *Sensors* **2021**, *21* (1), 115.
(2) Debéda, H.; Dufour, I. Resonant Microcantilever Devices for Gas Sensing. *Advanced Nanomaterials for Inexpensive Gas Microsensors*, 1st ed.; Elsevier: Amsterdam, 2020; pp 161−188.
(3) Vashist, S. K. A Review of Microcantilevers for Sensing Applications. *J. Nanotechnology* **2007**, *3*, 1−18.
(4) Zhao, L.; Huang, L.; Luo, G.; Wang, J.; Wang, H.; Wu, Y.; Li, Z.; Zhou, X.; Jiang, Z. An Immersive Resonant Sensor with Microcantilever for Pressure Measurement. *Sensors and Actuators A: Physical* **2020**, *303*, 111686.
(5) Ono, T.; Li, X.; Miyashita, H.; Esashi, M. Mass Sensing of Adsorbed Molecules in Sub-Picogram Sample with Ultrathin Silicon Resonator. *Review of scientific instruments* **2003**, *74* (3), 1240−1243.
(6) Wang, D. F.; Du, X.; Wang, X.; Ikehara, T.; Maeda, R. Improving Picogram Mass Sensitivity via Frequency Doubling in Coupled Silicon Micro-Cantilevers. *Journal of Micromechanics and Microengineering* **2016**, *26* (1), 015006.
(7) Verbridge, S. S.; Craighead, H. G.; Parpia, J. M. A Megahertz Nanomechanical Resonator with Room Temperature Quality Factor over a Million. *Appl. Phys. Lett.* **2008**, *92* (1), 013112.
(8) Ekinci, K. L.; Huang, X. M. H.; Roukes, M. L. Ultrasensitive Nanoelectromechanical Mass Detection. *Appl. Phys. Lett.* **2004**, *84* (22), 4469−4471.
(9) Sone, H.; Fujinuma, Y.; Hosaka, S. Picogram Mass Sensor Using Resonance Frequency Shift of Cantilever. *Jpn. J. Appl. Phys.* **2004**, *43* (6R), 3648.
(10) Bouchaala, A.; Nayfeh, A. H.; Younis, M. I. Frequency Shifts of Micro and Nano Cantilever Beam Resonators Due to Added Masses. *J. Dynamic Systems, Measurement, Control* **2016**, *138* (9), 091002.
(11) Gavan, K. B.; Van der Heijden, J.; Van der Drift, E. W.; Van der Zant, H. S. Effect of Pressure on the Q Factor and the Resonance Frequency of SiN Microcantilevers. *2009 4th IEEE International Conference on Nano/Micro Engineered and Molecular Systems*; IEEE: Washington, DC, 2009; pp 380−384.
(12) Bhiladvala, R. B.; Wang, Z. J. Effect of Fluids on the Q Factor and Resonance Frequency of Oscillating Micrometer and Nanometer Scale Beams. *Phys. Rev. E* **2004**, *69* (3), 036307.
(13) Bianco, S.; Cocuzza, M.; Ferrero, S.; Giuri, E.; Piacenza, G.; Pirri, C. F.; Ricci, A.; Scaltrito, L.; Bich, D.; Merialdo, A. Silicon Resonant Microcantilevers for Absolute Pressure Measurement. *J. Vac. Sci. Technol. A* **2006**, *24* (4), 1803−1809.
(14) Naeli, K.; Brand, O. Dimensional Considerations in Achieving Large Quality Factors for Resonant Silicon Cantilevers in Air. *J. Appl. Phys.* **2009**, *105* (1), 014908.
(15) Richter, G.; Hillerich, K.; Gianola, D. S.; Monig, R.; Kraft, O.; Volkert, C. A. Ultrahigh Strength Single Crystalline Nanowhiskers Grown by Physical Vapor Deposition. *Nano Lett.* **2009**, *9* (8), 3048−3052.
(16) Vogl, L. M.; Schweizer, P.; Pethö, L.; Sharma, A.; Spiecker, E.; Utke, I.; Michler, J. In Situ TEM Study to Unravel Dynamic Processes and Phase Transition During the Synthesis of Ultrathin Crystalline ALD Nanotubes. *Microscopy and Microanalysis* **2022**, *28* (S1), 2316−2318.
(17) Tian, M.; Wang, J.; Kurtz, J.; Mallouk, T.; Chan, M. Electrochemical Growth of Single-Crystal Metal Nanowires via a Two-Dimensional Nucleation and Growth Mechanism. *Nano Lett.* **2003**, *3*, 919−923.
(18) Wu, Y.; Xiang, J.; Yang, C.; Lu, W.; Lieber, C. M. Single-Crystal Metallic Nanowires and Metal/Semiconductor Nanowire Heterostructures. *Nature* **2004**, *430* (6995), 61−65.
(19) Vogl, L. M.; Schweizer, P.; Richter, G.; Spiecker, E. Effect of Size and Shape on the Elastic Modulus of Metal Nanowires. *MRS Advances* **2021**, *6* (27), 665−673.
(20) Lee, C. H.; Lee, S. W.; Lee, S. S. A Nanoradio Utilizing the Mechanical Resonance of a Vertically Aligned Nanopillar Array. *Nanoscale* **2014**, *6* (4), 2087−2093.
(21) Li, M.; Bhiladvala, R. B.; Morrow, T. J.; Sioss, J. A.; Lew, K.-K.; Redwing, J. M.; Keating, C. D.; Mayer, T. S. Bottom-up Assembly of Large-Area Nanowire Resonator Arrays. *Nature Nanotechnol.* **2008**, *3* (2), 88−92.
(22) Jensen, K.; Kim, K.; Zettl, A. An Atomic-Resolution Nanomechanical Mass Sensor. *Nature Nanotechnol.* **2008**, *3* (9), 533−537.
(23) Li, M.; Tang, H. X.; Roukes, M. L. Ultra-Sensitive NEMS-Based Cantilevers for Sensing, Scanned Probe and Very High-Frequency Applications. *Nature Nanotechnol.* **2007**, *2* (2), 114−120.
(24) Braakman, F. R.; Poggio, M. Force Sensing with Nanowire Cantilevers. *Nanotechnology* **2019**, *30* (33), 332001.
(25) Le Foulgoc, B.; Bourouina, T.; Le Traon, O.; Bosseboeuf, A.; Marty, F.; Breluzeau, C.; Grandchamp, J.-P.; Masson, S. Highly Decoupled Single-Crystal Silicon Resonators: An Approach for the Intrinsic Quality Factor. *J. Micromechanics Microeng.* **2006**, *16* (6), S45.
(26) Stifter, M.; Sachse, M.; Sauter, T.; Hortschitz, W.; Keplinger, F. Pressure Dependence of the Quality Factor of a Micromachined Cantilever in Rarefied Gases. *J. Phys.: Conf. Ser.* **2012**, *362*, 012033.
(27) Roy, S. K.; Sauer, V. T.; Westwood-Bachman, J. N.; Venkatasubramanian, A.; Hiebert, W. K. Improving Mechanical Sensor Performance through Larger Damping. *Science* **2018**, *360* (6394), eaar5220.
(28) Poncharal, P.; Wang, Z. L.; Ugarte, D.; Heer, W. A. de. Electrostatic Deflections and Electromechanical Resonances of Carbon Nanotubes. *Science* **1999**, *283* (5407), 1513−1516.
(29) Weisenburger, S.; Sandoghdar, V. Light Microscopy: An Ongoing Contemporary Revolution. *Contemporary Physics* **2015**, *56* (2), 123−143.
(30) Abbe, E. Beiträge Zur Theorie Des Mikroskops Und Der Mikroskopischen Wahrnehmung. *Archiv für mikroskopische Anatomie* **1873**, *9* (1), 413−468.
(31) Rayleigh, L. On the Theory of Optical Images, with Special Reference to the Microscope. *J. R. Microscop. Soc.* **1903**, *23* (4), 474−482.
(32) Martin, M. J.; Houston, B. H.; Baldwin, J. W.; Zalalutdinov, M. K. Damping Models for Microcantilevers, Bridges, and Torsional Resonators in the Free-Molecular-Flow Regime. *Journal of Microelectromechanical Systems* **2008**, *17* (2), 503−511.
(33) Zener, C. Internal Friction in Solids II. General Theory of Thermoelastic Internal Friction. *Physical review* **1938**, *53* (1), 90.
(34) Christian, R. G. The Theory of Oscillating-Vane Vacuum Gauges. *Vacuum* **1966**, *16* (4), 175−178.
(35) Newell, W. E. Miniaturization of Tuning Forks. *Science* **1968**, *161* (3848), 1320−1326.
(36) Blom, F. R.; Bouwstra, S.; Elwenspoek, M.; Fluitman, J. H. J. Dependence of the Quality Factor of Micromachined Silicon Beam Resonators on Pressure and Geometry. *Journal of Vacuum Science & Technology B: Microelectronics and Nanometer Structures Processing, Measurement, and Phenomena* **1992**, *10* (1), 19−26.
(37) Kádár, Z.; Kindt, W. J.; Bossche, A.; Mollinger, J. R. Quality Factor of Torsional Resonators in the Low-Pressure Region. *Sensors and Actuators A-physical* **1996**, *53*, 299−303.

https://doi.org/10.1021/acsnano.2c04848
ACS Nano 2022, 16, 18110−18118

(38) Li, P.; Hu, R. On the Air Damping of Flexible Microbeam in Free Space at the Free-Molecule Regime. *Microfluid. Nanofluid.* **2007**, *3* (6), 715−721.
(39) Jennings, S. G. The Mean Free Path in Air. *J. Aerosol Sci.* **1988**, *19* (2), 159−166.
(40) Memon, A.; Li, A.; Wencheng, H.; Tian, W. Effect of Gas Adsorption-Induced Pore Radius and Effective Stress on Shale Gas Permeability in Slip Flow: New Insights. *Open Geosci.* **2019**, *11*, 948−960.
(41) Vogl, L. M.; Schweizer, P.; Wu, M.; Spiecker, E. Transforming Layered MoS 2 into Functional MoO 2 Nanowires. *Nanoscale* **2019**, *11* (24), 11687−11695.
(42) Zach, M. P.; Inazu, K.; Ng, K. H.; Hemminger, J. C.; Penner, R. M. Synthesis of Molybdenum Nanowires with Millimeter-Scale Lengths Using Electrochemical Step Edge Decoration. *Chem. Mater.* **2002**, *14* (7), 3206−3216.
(43) Xu, S.; Qin, Y.; Xu, C.; Wei, Y.; Yang, R.; Wang, Z. L. Self-Powered Nanowire Devices. *Nat. Nanotechnol.* **2010**, *5* (5), 366−373.
(44) Tam, K. C.; Kubis, P.; Maisch, P.; Brabec, C. J.; Egelhaaf, H.-J. Fully Printed Organic Solar Modules with Bottom and Top Silver Nanowire Electrodes. *Progress in Photovoltaics: Research and Applications* **2022**, *30* (5), 528−542.
(45) Zhang, F.; Zhang, X.; Li, Z.; Yi, R.; Li, Z.; Wang, N.; Xu, X.; Azimi, Z.; Li, L.; Lysevych, M.; Gan, X.; Lu, Y.; Tan, H. H.; Jagadish, C.; Fu, L. A New Strategy for Selective Area Growth of Highly Uniform InGaAs/InP Multiple Quantum Well Nanowire Arrays for Optoelectronic Device Applications. *Adv. Funct. Mater.* **2022**, *32* (3), 2103057.
(46) Jo, M.-S.; Song, H.-J.; Kim, B.-J.; Shin, Y.-K.; Kim, S.-H.; Tian, X.; Kim, S.-M.; Seo, M.-H.; Yoon, J.-B. Aligned CuO Nanowire Array for a High Performance Visible Light Photodetector. *Sci. Rep.* **2022**, *12* (1), 2284.
(47) Ramgir, N. S.; Yang, Y.; Zacharias, M. Nanowire-Based Sensors. *Small* **2010**, *6* (16), 1705−1722.
(48) Cao, A.; Sudhölter, E. J. R.; De Smet, L. C. P. M. Silicon Nanowire-Based Devices for Gas-Phase Sensing. *Sensors* **2014**, *14* (1), 245−271.

https://doi.org/10.1021/acsnano.2c04848
ACS Nano 2022, 16, 18110−18118